World Journal of Radiology

Online Submissions: http://www.wjgnet.com/1949-8470office
wjr@wjgnet.com
doi:10.4329/wjr.v4.i4.167

World J Radiol 2012 April 28; 4(4): 167-173
ISSN 1949-8470 (online)

BRIEF ARTICLE

Virtual nonenhanced abdominal dual-energy MDCT: Analysis of image characteristics

Jacob Sosna, Shmuel Mahgerefteh, Liran Goshen, Galit Kafri, Galit Aviram, Arye Blachar

Jacob Sosna, Shmuel Mahgerefteh, Department of Radiology, Hadassah-Hebrew University Medical Center, Jerusalem 91120, Israel
Jacob Sosna, Department of Radiology, Beth Israel Deaconess Medical Center, Boston, MA 02215, United States
Liran Goshen, Galit Kafri, Philips Healthcare, Haifa 31004, Israel
Galit Aviram, Arye Blachar, Department of Radiology, Tel Aviv Sourasky Medical Center, Sackler School of Medicine, Tel Aviv University, Tel Aviv 64239, Israel
Author contributions: Sosna J guaranteed the integrity for this entire study; Sosna J and Blachar A contributed to study concepts and study design; Mahgerefteh S, Goshen L and Kafri G analysed data analysi; Sosna J, Aviram G, Mahgerefteh S and Blachar A drafted manuscript; all authors approved final revision.
Correspondence to: Jacob Sosna, MD, Department of Radiology, Hadassah Hebrew University Medical Center, POB 12000, Jerusalem 91120, Israel. jacobs@hadassah.org.il
Telephone: +972-2-6776901 Fax: +972-2-6776901
Received: October 28, 2011 Revised: February 20, 2012
Accepted: February 27, 2012
Published online: April 28, 2012

Abstract

AIM: To evaluate abdominal and pelvic image characteristics and artifacts on virtual nonenhanced (VNE) images generated from contrast-enhanced dual-energy multidetector computed tomography (MDCT) studies.

METHODS: Hadassah-Hebrew University Medical Institutional Review Board approval was obtained; 22 patients underwent clinically-indicated abdominal and pelvic single-source dual-energy MDCT (Philips Healthcare, Cleveland, OH, USA), pre- and post-IV administration of Omnipaque 300 contrast (100 cc). Various solid and vascular structures were evaluated. VNE images were generated from the portal contrast-enhanced phase using probabilistic separation. Contrast-enhanced-, regular nonenhanced (RNE)-, and VNE images were evaluated with a total of 1494 density measurements. The ratio of iodine contrast deletion was calculated. Visualization of calcifications, urinary tract stones, and image artifacts in VNE images were assessed.

RESULTS: VNE images were successfully generated in all patients. Significant portal-phase iodine contrast deletion was seen in the kidney (61.7%), adrenal gland (55.3%), iliac artery (55.0%), aorta (51.6%), and spleen (34.5%). Contrast deletion was also significant in the right atrium (RA) (51.5%) and portal vein (39.3%), but insignificant in the iliac vein and inferior vena cava (IVC). Average post contrast-to-VNE HU differences were significant ($P < 0.05$) in the: RA -135.3 (SD 121.8), aorta -114.1 (SD 48.5), iliac artery -104.6 (SD 53.7), kidney -30.3 (SD 34.9), spleen -9.2 (SD 8.8), and portal vein -7.7 (SD 13.2). Average VNE-to-RNE HU differences were significant in all organs but the prostate and subcutaneous fat: aorta 38.0 (SD 9.3), RA 37.8 (SD 16.1), portal vein 21.8 (SD 12.0), IVC 12.2 (SD 11.6), muscle 3.3 (SD 4.9), liver 5.7 (SD 6.4), spleen 22.3 (SD 9.8), kidney 40.5 (SD 6.8), and adrenal 20.7 (SD 13.5). On VNE images, 196/213 calcifications (92%) and 5/6 renal stones (84%) were visualized. Lytic-like artifacts in the vertebral bodies were seen in all studies.

CONCLUSION: Iodine deletion in VNE images is most significant in arteries, and less significant in solid organs and veins. Most vascular and intra-abdominal organ calcifications are preserved.

Key words: Abdominal computed tomography; Dual-energy computed tomography; Pelvic computed tomography; Virtual nonenhanced computed tomography

Peer reviewer: Filippo Cademartiri, MD, PhD, Departmento of Radiology - c/o Piastra Tecnica - Piano 0, Azienda Ospedaliero-Universitaria di Parma, Via Gramsci, 14 - 43100 Parma, Italy

Sosna J, Mahgerefteh S, Goshen L, Kafri G, Aviram G, Blachar A. Virtual nonenhanced abdominal dual-energy MDCT: Analysis of image characteristics. *World J Radiol* 2012; 4(4): 167-173 Available from: URL: http://www.wjgnet.com/1949-8470/full/v4/i4/167.htm DOI: http://dx.doi.org/10.4329/wjr.v4.i4.167

INTRODUCTION

The past years have been characterized by tremendous progress in computed tomography (CT) technology. With the introduction of multidetector (MD) scanners that produce very high quality images, CT use has increased markedly. Recently, MDCT and dual-energy imaging capabilities were combined. Dual-energy techniques are designed to capture information from varying responses of materials with a range of Compton and photoelectric effects to X-rays at different energies[1].

Dual-energy acquisition enables reconstruction of virtual nonenhanced (VNE) images, wherein the iodine content of contrast-enhanced CT images is subtracted using image post-processing techniques[2]. VNE images have been shown to be useful in various clinical settings, ranging from the detection of masses and stones to evaluation of vascular disease[3]. The virtual deletion of iodine is appealing, as it may obviate the need for the nonenhanced imaging phase in multiphase studies; thus, VNE has the potential to significantly reduce X-ray exposure for patients and shorten CT study times[3].

To the best of our knowledge, a comparative evaluation of VNE at the various abdominal and pelvic organs has never been carried out. We aimed to systematically evaluate VNE images generated from a dual-energy multi-detector CT using probabilistic separation and a VNE algorithm, and to assess iodine contrast deletion, depiction of calcifications, and extent of image artifacts in abdominal and pelvic scans.

MATERIALS AND METHODS

Authors who are not employees of Philips Healthcare (JS, SM, GA, AB) had continuous control of all information and research data in this study, with JS acting as the guarantor of integrity for the entire study.

The dual-energy CT system

The study was performed on a prototype single-source dual-energy MDCT available for research purposes (Philips Healthcare, Cleveland, OH, USA). The scanner tube was conventional, without modulation capabilities. Dual-energy was based on dual detector capability, with the upper layer primarily absorbing the lower X-ray energy spectrum, and the lower detector layer absorbing the remainder of the spectrum, mainly in the higher energy range[4]. Each layer has 32 detector rows and a 50 cm full field-of-view. Data from each layer, corresponding to lower- and higher energies, are independently reconstructed. In addition, a combined standard CT image is reconstructed from weighted raw signals of the two layers. As the evaluated scanner is based on a single-source dual-energy layer, a single kVp is provided, with separation of the low- and high-energy images at the detector level.

Study population

Hadassah-Hebrew University Medical Institutional Review Board approval was obtained. All participants had clinical indications for abdominal and pelvic CT, and signed an informed consent. The consent form included information on the research scanner and a statement that radiological interpretation would be based solely on the conventional averaged CT image. Twenty-two consecutive patients referred for clinically indicated CT studies were included in the study, including eight women and 14 men ranging in age from 38-71 years (mean 60 years, SD 10 years). CT studies were performed using collimation of 32 × 0.625 mm, FOV of 50 cm, slice thickness and increment of 1-3 mm, 140 kVp, 250-300 mAs, and kernel B. Air calibration was performed before each scan.

All patients were scanned before and after intravenous administration of 100 cc of iohexol (Omnipaque 300, Amersham Health, Princeton NJ, USA), injected at a rate of 3-4 cc/s using a mechanical injector (Medrad, Warrendale, PA, USA). Scans were performed within 60 s from initiation of injection.

Solid organs evaluated were subcutaneous fat, erecter spinae muscle, spleen, liver, adrenal gland, kidney, and prostate. Vascular structures evaluated were the right atrium (RA), aorta, inferior vena cava (IVC), portal vein, common iliac artery and vein, external iliac artery and vein, and common femoral artery and vein.

VNE generation technique

The analysis consisted of two steps[2]: (1) estimation of material response vectors; and (2) iodine-calcium separation. The first step was accomplished using an automatic algorithm that estimated the material response vectors of iodine, calcium, and soft tissue on the dual-energy map. This algorithm was applied for each slice in the study to eliminate beam-hardening effects that may impact on the orientation of material response vectors. The algorithm presented the distribution of voxel distance from material response vectors in the energy map as a probability model to estimate combinations of iodine, calcium, and soft tissue voxels.

The second step was implemented using a separation algorithm to estimate the probability for each voxel to be either iodine or calcium. The algorithm incorporated the estimated response vectors to approximate prior probabilities that iodine or calcium were depicted in each region of the volume.

Systematic image analysis

CT scans were loaded on a Kodak PACS viewing station (Carestream Health, Rochester NY, USA). Contrast enhanced-, regular nonenhanced (RNE)-, and VNE images were evaluated separately using the combined weighted CT for the RNE and contrast enhanced studies. Multiple attenuation measurements were performed on various organs. Measurements were performed by a research fellow with 12 mo experience in dual-energy CT (SM) using regions-of-interest (ROI) that were identical in size and location on all VNE and RNE images. ROI measurements of organs were obtained with care to avoid calcifi-

cations and vessels within the organs, as well as obvious masses. ROI size varied from 0.7 to 2.5 cm^2. Standard deviations were calculated for each measurement. A total of 1494 density measurements were performed, including 22 measurements in each female patient, and 23 for each male patient, including the prostate.

Densities were measured in the RA and in a number of vessels, including the aorta, IVC, main portal vein, right common iliac and right external iliac artery and vein, and right common femoral artery and vein. Multiple intra-abdominal organ densities were measured, including the right hepatic lobe (at the level of the right portal vein), left hepatic lobe (at the level of the left portal vein), spleen (at the level of the splenic hilum), prostate, left adrenal, right kidney (cortex, at a subcapsular location), left erector spinae muscle, and right posterior subcutaneous fat.

Evaluation of virtual contrast deletion: To determine the difference in attenuation between VNE- and post contrast images, we subtracted attenuation values measured on VNE images from values on images showing contrast enhancement. To determine the difference in attenuation between VNE- and RNE images, we subtracted attenuation values measured on VNE images from values on the RNE images. We calculated the average difference for each measured area. The ratio of these two subtractions was then calculated to generate the percentage of contrast deletion, defined as (contrast-VNE)/(contrast-NE).

Calcifications and urinary stones: The presence of organ calcifications and urinary stones was evaluated in consensus by two experienced abdominal radiologists (AB and JS) with 14 and 12 years of experience, respectively. Each organ calcification identified in an RNE image was evaluated on the VNE images as still visible or completely deleted in comparison to the RNE study. Since there is no accurate system enabling precise evaluation of the change in aortic calcifications on VNC images, we evaluated these calcifications subjectively. The most heavily calcified 5 cm section of each vessel was chosen. Calcifications seen on RNE and VNE images were measured, including calcifications in arterial walls, as well as intraluminal densities of arteries and veins. Urinary stones were assessed separately.

Artifacts: The presence and nature of artifacts on VNE images were evaluated to identify focal changes in VNE image quality that were not seen on the RNE image and that were not anatomical or pathological.

Statistical analysis

Descriptive statistics were used where appropriate. The sign test was used to compare the differences in attenuation between contrast enhanced-, RNE-, and VNE images to test the hypothesis that there is no difference between RNE and VNE in a situation when paired samples could be drawn. All analyses were performed with SAS statistical analysis software (version 9.1, SAS Institute, Cary NC, USA). $P < 0.05$ was considered significant.

Table 1 Subtraction of the average HU measurements of organs evaluated: Enhanced computed tomography minus virtual nonenhanced images

Organ	mean ± SD	*P* value	Percent deletion
Adrenal gland	1.8 ± 6.9	< 0.0001	55.3
Kidney	30.279 ± 34.91	< 0.0001	61.7
Spleen	9.202 ± 8.79	< 0.0001	34.5
Liver	3.619 ± 9.21	0.490	10.2
Subcutaneous fat	0.330 ± 2.52	0.8318	2.3
Prostate	-0.183 ± 1.63	1.0000	13.3
Erector spinae muscle	-0.403 ± 2.64	0.5235	7.7
Right atrium	135.4 ± 16.0	< 0.0001	51.5
Portal vein	7.6 ± 2.3	0.0015	39.3
Inferior vena cava	1.7 ± 2.0	0.5235	26.6
Aorta	114.1 ± 1.2	< 0.0001	51.6
Iliac vein	3.616 ± 3.04	0.0625	25.3
Iliac artery	104.64 ± 53.66	< 0.0001	55.0

RESULTS

Contrast deletion

VNE images were generated successfully in all 22 patients, using probabilistic separation. Evaluation of the RA and multiple intra-abdominal organ and vascular densities showed that contrast deletion was indeed substantial (Table 1). Contrast material deletion was significant at 51.6% and 55.0% in the aorta and iliac artery, respectively. Among the veins, only the portal vein showed statistically significant deletion, at 39.3%; deletions at the IVC and iliac vein were both insignificant at around 25%, however, the RA showed significant deletion at 51.5%. Intra-abdominal organs demonstrating significant contrast deletion were spleen (34.5%), adrenal (55.3%) and the kidney at the portal phase (61.7%) (Figure 1). Deletion in the prostate was about 13% and insignificant. Deletion was heterogeneous and insignificant in the liver, averaging about 10% overall. Subcutaneous tissues and muscles showed the least contrast enhancement, as well as the lowest degree of contrast deletion.

The differences in density between RNE and VNE are shown in Table 2. These differences were statistically significant for all organs but the iliac vein, prostate, erector spinae muscle, and subcutaneous fat. Among solid intra-abdominal organs, the mean differences ranged between 20-40 HU for the kidney, adrenal and spleen ($P < 0.001$) and did not exceed 6 HU for the liver ($P < 0.01$). For vessels, deletion ranged from 8.3 HU for the iliac vein ($P = 0.02$) to about 38 HU for the RA, aorta and iliac artery ($P < 0.0001$).

Organ and vascular calcifications

Evaluation of the arteries on RNE studies revealed 213 calcifications, of which 196 (92%) were visualized on the VNE images (Figure 2). There were six renal stones ranging in size from 1-8 mm. Only one renal stone, 2 mm in

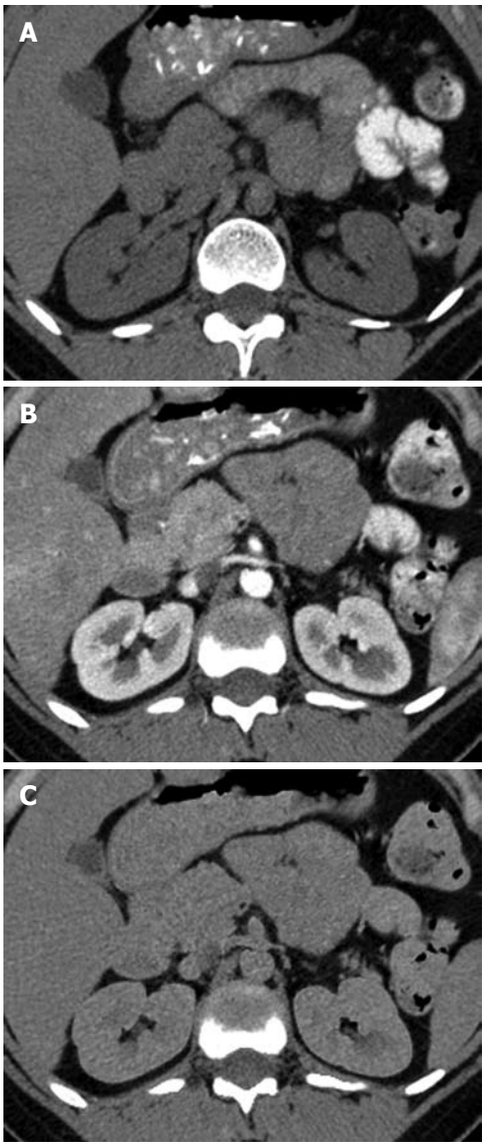

Figure 1 A 52-year-old female with the kidney contrast deletion. A, B: The regular nonenhanced (A) and contrast-enhanced (B) images demonstrate kidneys with normal appearance; C: Virtual nonenhanced shows substantial deletion of contrast from the kidney parenchyma.

Table 2 Average HU differences in densities of organs evaluated on virtual nonenhanced minus regular nonenhanced images

Organ	mean ± SD	*P* value
Adrenal gland	20.7 ± 13.5	< 0.0001
Kidney	40.5 ± 6.8	< 0.0001
Spleen	22.3 ± 9.8	< 0.0001
Liver	5.8 ± 6.9	0.0072
Subcutaneous fat	-0.3 ± 4.54	1.0000
Prostate	4.3 ± 6.6	0.5000
Erector spinae muscle	3.3 ± 4.9	0.0169
Right atrium	37.8 ± 16.1	< 0.0001
Portal vein	21.8 ± 12.0	0.0002
Inferior vena cava	12.2 ± 11.6	< 0.0001
Aorta	38.0 ± 9.3	< 0.0001
Iliac vein	8.3 ± 7.9	0.0225
Iliac artery	38.4 ± 15.0	< 0.0001

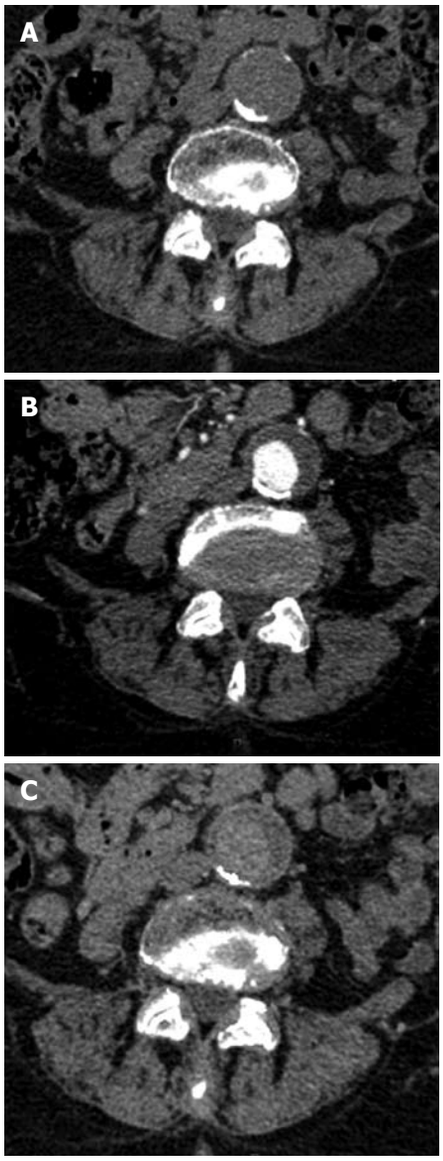

Figure 2 A 60-year-old male with an abdominal aortic aneurysm. A: Regular nonenhanced image demonstrates a curved calcification in the posterior border of the aneurysm with some smaller calcifications in the anterior border; B: The contrast enhanced image shows opacification of the lumen; C: Virtual nonenhanced shows preserved posterior calcifications with deletion of the smaller anterior calcifications.

diameter, was deleted on VNE images; other stones were visible and only partially deleted (Figure 3).

Artifacts

Artifacts were seen in all VNE studies. In the vertebral bodies, they were seen as lytic-like lesions. These were easily identified as artifacts and were not expected to cause the VNE studies to be non-diagnostic (Figure 4).

DISCUSSION

Before the use of VNE imaging becomes widespread, a systematic comparative evaluation of the characteristics of iodine deletion and artifacts at various abdominal or-

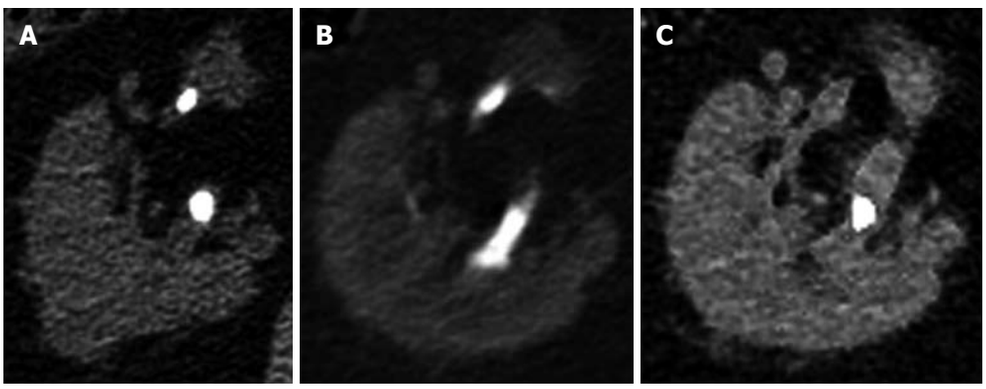

Figure 3 Regular nonenhanced image (A) demonstrates two stones in the right kidney of a 64-year-old male. B: In the contrast-enhanced image, contrast excretion into the collecting system is inhibited by the stones, which are obscured; C: In the virtual nonenhanced image, the posterior stone is maintained while the anterior stone is deleted.

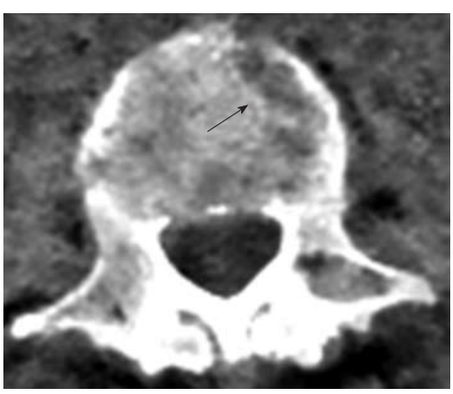

Figure 4 Virtual nonenhanced image of this 58-year-old female shows a lytic-like artifact in the vertebral body. The "lesion" was easily identified as an artifact.

gans is important to assess the clinical potential of these studies for specific applications. Our study demonstrates the technical feasibility and imaging characteristics of VNE images. In this series, iodine deletion reached as high as 50%-60% in arterial vessels, RA, adrenal and kidney. It was less pronounced in veins and in the remaining abdominal organs. The majority of vascular calcifications and renal stones were preserved. Specific, easily recognized artifacts could be attributed to this technique.

The importance of noncontrast imaging as a part of CT protocols has been shown previously[5]. At CT angiography, a noncontrast study is usually obtained first to identify high attenuation in the aortic wall, which is consistent with intramural hematoma and may indicate early or impending rupture. Noncontrast images are also useful in evaluating and defining high attenuating structures such as calcium or metal that may be confused with enhancement on post-contrast images, for example in patients evaluated after abdominal aortic aneurysm repair.

Noncontrast images of the liver are used to demonstrate calcifications and fibrosis, and to provide important information in the characterization of hepatic masses[6]. In the kidneys, noncontrast images are used to detect the presence of calcifications and their degree of enhancement[7]. Imaging and characterization of adrenal masses also currently relies on noncontrast image acquisition[8]. Multiphasic imaging of the liver, pancreas, kidney and thorax has therefore become standard practice[9].

Recently, it has been shown that dual-energy dual-source CT scans performed during the delayed phase, with reconstruction of VNE images, enables detection of endoleaks after endovascular abdominal aortic aneurysm repair with high accuracy and a considerably lower patient radiation dose[10-12]. Chow *et al*[11] have shown that 94% of VNE images are diagnostic; similarly, in our study, all images were diagnostic. The Sommer group reported at least minimal subtraction of calcifications in 70% of their VNE images[11], whereas we found only 8% subtraction. This difference might be attributed to differences in the dual-energy algorithms used for iodine deletion from the CT images.

VNE imaging has already been used in the characterization of pulmonary nodules. Chae *et al*[13] reported detection of 85.0% of calcifications (17 of 20) in solitary pulmonary nodules and 97.8% of calcifications (44 of 45) in the lymph nodes on VNE images, although apparent size was smaller on VNE- compared with non-enhanced weighted average images. These results are in accordance with our findings in relation to the preservation of calcifications.

Dual-energy contrast-enhanced CT acquisition with VNE reformation has shown sensitivity, specificity, and positive- and negative predictive values of 83%, 100%, 100%, and 88%, respectively, for the detection of urinary stone disease[14]. In our study, most urinary stones were also preserved. This may be beneficial in CT urography studies, since it may enable stone detection with omission of the nonenhanced phase.

Graser *et al*[15] have shown the reliability of VNE imaging for assessment of renal masses with similar density on VNE and RNE images. In our study, however, there were differences in density on VNE and RNE images of the kidney. This may be attributable to differences in timing of contrast injection, and the use of different dual-energy scanning techniques; Graser *et al*[15] used a

dual-source, while we used a dual-detector scanner in our study. On the other hand, differences in liver density on VNE and RNE images were minimal in our study; thus VNE may be performed in the future to avoid the need for a nonenhanced phase in multi-phasic liver studies. Zhang *et al*[16] showed that arterial- and portovenous-phase-derived VNE images can detect 91% and 81% of focal liver lesions, respectively.

The ability of DECT-derived VNE images to depict urinary stones in an iodine solution was tested in a phantom model[17]. Stone visibility rates varied with changes in iodine concentration and kVp. The study showed that VNE is capable of depicting urinary stones in iodine solutions of a diverse range of concentrations in a phantom study. With regard to urinary stones, our *in vivo* study supports the findings obtained in a phantom model from this earlier study.

Since contrast deletion occurred mainly from arteries in our study, it would seem more logical to perform VNE algorithms at the arterial phase rather than the venous phase, when there is also less iodine in the parenchyma. Compared to the portal venous phase, the hepatic arterial phase of dual-energy VNE was shown to provide better image quality and may be more diagnostic[16,18]. The reason for the improved contrast deletion from arteries is probably related to the higher iodine concentration within vessels with higher HU values, and more specifically within the pixels with iodine content. Further phantom and clinical studies are needed to assess differences in VNE images derived from the arterial and venous phases, as well as variation due to differences in deletion algorithms.

VNE has the potential to significantly decrease patient exposure to ionizing radiation, an issue of increasing concern. The National Council on Radiation Protection and Measurements estimates that the annual medical radiation dose in the general population has increased by a factor of nearly six since the early 1980s[19,20]. The number of CT scans performed in the US increased from 18.3 million in 1993 to 67 million in 2006[20]. It is estimated that CT scans constituted only 17% of all medical radiation procedures, but contributed about 49% of the collective dose in 2006[20].

In the past decade, both the clinical utility and the availability of CT have increased significantly, resulting in a dramatic increase in CT utilization[21]. It is thus important that patient radiation exposure is carefully considered, particularly in the case of multiphasic, repeated, or multiple examinations[22-25]. Further study of the clinical role for VNE reformation would thus appear to be a high priority. Depending on the setting in which it is implicated, VNE has the potential to reduce radiation dose by as much as 60% in a single study[3].

There are some limitations to our study. The population was relatively small. We have also evaluated only one type of dual-energy scanner. Other techniques for dual-energy CT imaging may yield different levels of iodine contrast deletion; acquisition techniques and reformation algorithms are unique for each commercially available system. It should also be noted that our RNE images were weighted averages of dual-energy datasets, derived from DECT technology with the unique capability for simultaneous dual- and single-energy image construction following a single scan. In theory, our RNE images should represent true single-scan data, however, it is possible that comparison of our VNE images to RNE images acquired at conventional MDCT might yield different results than those described here.

In conclusion, VNE images can be obtained with dual energy CT, with iodine mainly deleted from arteries and solid organs rich in blood supply such as the kidneys, adrenal gland, and spleen. A lesser degree of iodine deletion is seen in other abdominal solid organs such as the liver, as well as in the veins. Most vascular and intra-abdominal organ calcifications are preserved. VNE technology may potentially obviate the need for RNE image acquisition when multi-phase studies are needed, thereby reducing the overall radiation burden, but this must be investigated further in abdominal organs.

ACKNOWLEDGMENTS

Jacob Sosna, Professor is the principle investigator under a research agreement with Philips HealthCare. Dr. Liran Goshen and Dr. Galit Kafri are employees of Philips HealthCare. The other authors have no conflicts of interest to disclose.

The authors wish to thank Shifra Fraifeld, MBA, a Research Associate in the Department of Radiology at Hadassah Medical Center, for her contribution to database development and management, and her editorial assistance in the preparation of this manuscript.

COMMENTS

Background

Dual-energy acquisition enables reconstruction of virtual nonenhanced (VNE) images, wherein the iodine content of contrast-enhanced computed tomography (CT) images is subtracted using image post-processing techniques. VNE images have been shown to be useful in various clinical settings, ranging from detection of masses and stones to evaluation of vascular disease. The virtual deletion of iodine is appealing, as it may obviate the need for the nonenhanced imaging phase in multiphase studies; thus, VNE has the potential to significantly reduce X-ray exposure for patients and shorten CT study times.

Research frontiers

The paper aimed to systematically evaluate VNE images generated from a dual-energy multidetector CT (MDCT) using probabilistic separation and a VNE algorithm, and to assess iodine contrast deletion, depiction of calcifications, and extent of image artifacts in abdominal and pelvic scans.

Innovations and breakthroughs

The study demonstrates the technical feasibility and imaging characteristics of VNE images. In this series, iodine deletion reached as high as 50%-60% in arterial vessels, right atrium, adrenal and kidney. It was less pronounced in veins and in the remaining abdominal organs. The majority of vascular calcifications and renal stones were preserved. Specific artifacts could be attributed to this technique, and these were easily recognized as such. All images were diagnostic, with only 8% of calcifications being subtracted. In previous series, findings in renal parenchyma showed similar density on VNE and regular nonenhanced (RNE) images. In the study, however, there were differences in density on VNE and RNE images of the kidney. This may be attributable to differences in timing

of contrast injection, and the use of different dual-energy scanning techniques. On the other hand, differences in liver density on VNE and RNE images were minimal in the study; thus VNE may be performed in the future to avoid the need for a nonenhanced phase in multi-phasic liver studies. Since contrast deletion occurred mainly from arteries in our study, it would seem more logical to perform VNE algorithms at the arterial phase rather than the venous phase, when there is also less iodine in the parenchyma. Compared to the portal venous phase, the hepatic arterial phase of dual-energy VNE has been previously shown to provide better image quality and may be more diagnostic.

Applications

VNE images can be obtained with dual-energy CT, with iodine mainly deleted from arteries and solid organs rich in blood supply such as the kidney, adrenal gland, and spleen. A lesser degree of iodine deletion is seen in other abdominal solid organs such as the liver, as well as in the veins. Most vascular and intra-abdominal organ calcifications are preserved. VNE technology may potentially obviate the need for RNE image acquisition in abdominal imaging when multi-phase studies are needed, thereby reducing the overall radiation burden.

Terminology

Dual-energy CT: An emerging CT imaging technique in which two datasets are obtained at a single scan, corresponding to two distinct energy spectra; these distinct datasets are then analyzed to reveal material-specific information. VNE image: An image derived from postprocessing of data acquired at dual-energy CT, in which iodinated contrast material is digitally deleted from the original contrast-enhanced image.

Peer review

This study represents an important step in the advancement of dual-energy CT in general and VNE imaging in particular. While other VNE studies have focused on specific organs or disease entities, this study provides the first comprehensive demonstration of the clinical feasibility and utility of VNE imaging within the abdomen as a whole. The results presented here support the advancement of this unique imaging technique in abdominal imaging, whereby radiation exposure to patients can be dramatically reduced. Further studies should compare the performances of the various dual-energy data acquisition systems and VNE algorithms in the abdomen.

REFERENCES

1 **Avrin DE**, Macovski A, Zatz LE. Clinical application of Compton and photo-electric reconstruction in computed tomography: preliminary results. *Invest Radiol* 1978; **13**: 217-222
2 **Goshen L**, Sosna J, Carmi R, Kafri G, Iancu I, Altman A. An iodine-calcium separation analysis and virtually non-contrasted image generation obtained with single source dual energy MDCT. *IEEE Nucl Sci Symp Conf Rec* 2008; 3868-3870
3 **Mahgerefteh S**, Blachar A, Fraifeld S, Sosna J. Dual-energy derived virtual nonenhanced computed tomography imaging: current status and applications. *Semin Ultrasound CT MR* 2010; **31**: 321-327
4 **Carmi R**, Naveh G, Altman A. Material separation with dual-layer CT. *IEEE Nuclear Sci Symp Conf Rec* 2005; **4**: 1876-1878
5 **Bhalla S**, Menias CO, Heiken JP. CT of acute abdominal aortic disorders. *Radiol Clin North Am* 2003; **41**: 1153-1169
6 **Federle MP**, Blachar A. CT evaluation of the liver: principles and techniques. *Semin Liver Dis* 2001; **21**: 135-145
7 **Yuh BI**, Cohan RH. Different phases of renal enhancement: role in detecting and characterizing renal masses during helical CT. *AJR Am J Roentgenol* 1999; **173**: 747-755
8 **Korobkin M**, Francis IR. Imaging of adrenal masses. *Urol Clin North Am* 1997; **24**: 603-622
9 **Tatli S**, Yucel EK, Lipton MJ. CT and MR imaging of the thoracic aorta: current techniques and clinical applications. *Radiol Clin North Am* 2004; **42**: 565-585, vi
10 **Stolzmann P**, Frauenfelder T, Pfammatter T, Peter N, Scheffel H, Lachat M, Schmidt B, Marincek B, Alkadhi H, Schertler T. Endoleaks after endovascular abdominal aortic aneurysm repair: detection with dual-energy dual-source CT. *Radiology* 2008; **249**: 682-691
11 **Chow LC**, Kwan SW, Olcott EW, Sommer G. Split-bolus MDCT urography with synchronous nephrographic and excretory phase enhancement. *AJR Am J Roentgenol* 2007; **189**: 314-322
12 **Chandarana H**, Godoy MC, Vlahos I, Graser A, Babb J, Leidecker C, Macari M. Abdominal aorta: evaluation with dual-source dual-energy multidetector CT after endovascular repair of aneurysms--initial observations. *Radiology* 2008; **249**: 692-700
13 **Chae EJ**, Song JW, Seo JB, Krauss B, Jang YM, Song KS. Clinical utility of dual-energy CT in the evaluation of solitary pulmonary nodules: initial experience. *Radiology* 2008; **249**: 671-681
14 **Scheffel H**, Stolzmann P, Frauenfelder T, Schertler T, Desbiolles L, Leschka S, Marincek B, Alkadhi H. Dual-energy contrast-enhanced computed tomography for the detection of urinary stone disease. *Invest Radiol* 2007; **42**: 823-829
15 **Graser A**, Johnson TR, Hecht EM, Becker CR, Leidecker C, Staehler M, Stief CG, Hildebrandt H, Godoy MC, Finn ME, Stepansky F, Reiser MF, Macari M. Dual-energy CT in patients suspected of having renal masses: can virtual nonenhanced images replace true nonenhanced images? *Radiology* 2009; **252**: 433-440
16 **Zhang LJ**, Peng J, Wu SY, Wang ZJ, Wu XS, Zhou CS, Ji XM, Lu GM. Liver virtual non-enhanced CT with dual-source, dual-energy CT: a preliminary study. *Eur Radiol* 2010; **20**: 2257-2264
17 **Takahashi N**, Hartman RP, Vrtiska TJ, Kawashima A, Primak AN, Dzyubak OP, Mandrekar JN, Fletcher JG, McCollough CH. Dual-energy CT iodine-subtraction virtual unenhanced technique to detect urinary stones in an iodine-filled collecting system: a phantom study. *AJR Am J Roentgenol* 2008; **190**: 1169-1173
18 **Peng J**, Zhang LJ, Wu S, Lu GM. A preliminary study of epigastrium dual energy virtual noncontrast CT of dual source CT. Chicago, IL: Radiological Society of North America, 2009
19 **National Council on Radiation Protection and Measurements**. Ionizing Radiation Exposure of the Population of the United States. Bethesda, MD: National Council on Radiation Protection and Measurements, 2009
20 **Mettler FA**, Thomadsen BR, Bhargavan M, Gilley DB, Gray JE, Lipoti JA, McCrohan J, Yoshizumi TT, Mahesh M. Medical radiation exposure in the U.S. in 2006: preliminary results. *Health Phys* 2008; **95**: 502-507
21 **Huda W**, Vance A. Patient radiation doses from adult and pediatric CT. *AJR Am J Roentgenol* 2007; **188**: 540-546
22 **Catalano C**, Francone M, Ascarelli A, Mangia M, Iacucci I, Passariello R. Optimizing radiation dose and image quality. *Eur Radiol* 2007; **17** Suppl 6: F26-F32
23 **Fazel R**, Krumholz HM, Wang Y, Ross JS, Chen J, Ting HH, Shah ND, Nasir K, Einstein AJ, Nallamothu BK. Exposure to low-dose ionizing radiation from medical imaging procedures. *N Engl J Med* 2009; **361**: 849-857
24 **Frush DP**. Review of radiation issues for computed tomography. *Semin Ultrasound CT MR* 2004; **25**: 17-24
25 **Valentin J**. Managing patient dose in multi-detector computed tomography(MDCT). ICRP Publication 102. *Ann ICRP* 2007; **37**: 1-79, iii

S- Editor Cheng JX **L- Editor** Webster JR **E- Editor** Zheng XM